Inorg. Chem. **2007**, *46*, 6837−6839

Synthesis and Magnetic Properties of a Highly Conducting Neutral Nickel Complex with a Highly Conjugated Tetrathiafulvalenedithiolate Ligand

He-Rui Wen,[†] Cheng-Hui Li,[†] You Song,[†] Jing-Lin Zuo,*[,†] Bin Zhang,*[,‡] and Xiao-Zeng You[†]

Coordination Chemistry Institute and the State Key Laboratory of Coordination Chemistry, School of Chemistry and Chemical Engineering, Nanjing University, Nanjing 210093, China, and Organic Solid Laboratory, CMS, Institute of Chemistry, Beijing 100080, China

Received February 10, 2007

A neutral nickel complex with the extended tetrathiafulvalene-4,5-dithiolate ligand benzotetrathiafulvalenedithiolate ($btdt^{2-}$) is synthesized and characterized. From the structural analysis, the neighboring molecules in this complex are stacked in a different way compared to the previously reported single-component metal [$Ni(tmdt)_2$]. The computational studies confirm that the difference in molecular packing results in the variance of conductivity.

Metal complexes of multiple-sulfur 1,2-dithiolene ligands have been extensively studied as materials for molecular conductors and superconductors.[1−4] Intermolecular interactions through shorter S−S contacts are the basic requirement for high conductivity. Recently, metal complexes containing extended tetrathiafulvalenedithiolene (tetrathisfulvalene = TTF) ligands have been of great interest because of their possible extended π-conjugation system and better electrical conduction properties.[2−4] The three-dimensional synthetic metal composed of single-component planar molecules $Ni(tmdt)_2$ (tmdt = trimethylenetetrathiafulvalenedithiolate) exhibited an extremely high electrical conductivity (400 S cm^{-1}) at room temperature.[3c] However, in these metal complexes with extended tetrathiafulvalenedithiolate ligands, the extended sections on the TTF framework are all alkyl groups. Usually, bulky alkyl groups on the TTF framework will lead to the molecules packing in a noncompact manner, which decreases the intermolecular interaction. Therefore, the introduction of π-conjugated groups, such as a phenyl group, on the TTF framework may show great effects on the conducting properties of the resulting complexes. We report herein the synthesis and properties of a highly conducting neutral nickel complex with a π-conjugated dithiolate ligand, [$Ni(btdt)_2$] (btdt = benzotetrathiafulvalenedithiolate; Scheme 1).

The neutral complex [$Ni(btdt)_2$] was prepared according to the literature methods (see the Supporting Information for details). It is insoluble in common organic solvents, thus making it difficult to get the single-crystal suitable for the structure determination. However, we can solve the crystal structure from powder X-ray diffraction (PXRD) data using the Rietveld refinement technique.[5,6] Details of the structure determination are described in the Supporting Information. The final Rietveld refinement plot is shown in Figure S1.

* To whom correspondence should be addressed. E-mail: zuojl@nju.edu.cn (J.L.Z.), zhangbin@iccas.ac.cn (B.Z.).
[†] Nanjing University.
[‡] Institute of Chemistry.

(1) Williams, J. M.; Ferraro, J. R.; Thorn, R. J.; Carson, K. D.; Geiser, U.; Wang, H. H.; Kini, A. M.; Whangbo, M.-H. *Organic Superconductors*; Prentice Hall: Englewood Cliffs, NJ, 1992.
(2) (a) Kobayashi, A.; Tanaka, H.; Kobayashi, H. *J. Mater. Chem.* **2001**, *11*, 2078−2088. (b) Robertson, N.; Cronin, L. *Coord. Chem. Rev.* **2002**, *227*, 93−127. (c) Kobayashi, A.; Fujiwara, E.; Kobayashi, H. *Chem. Rev.* **2004**, *104*, 5243−5264. (d) Kobayashi, A.; Zhou, B.; Kobayashi, H. *J. Mater. Chem.* **2005**, *15*, 3449−3451. (e) Kobayashi, A.; Kobayashi, H. *Mol. Cryst. Liq. Cryst.* **2006**, *455*, 47−56.
(3) (a) Narvor, N. L.; Robertson, N.; Weyland, T.; Killburn, J. D.; Underhill, A. E.; Webster, M.; Svenstrup, N.; Becker, J. *J. Chem. Soc., Chem. Commun.* **1996**, 1363−1364. (b) Kobayashi, A.; Tanaka, H.; Kumasaki, M.; Torii, H.; Narymbetov, B.; Adachi, T. *J. Am. Chem. Soc.* **1999**, *121*, 10763−10771. (c) Tanaka, M.; Okano, Y.; Kobayashi, H.; Suzuki, W.; Kobayashi, A. *Science* **2001**, *291*, 285−287. (d) Tanaka, H.; Kobayashi, H.; Kobayashi, A. *J. Am. Chem. Soc.* **2002**, *124*, 10002−10003. (e) Kobayashi, A.; Sasa, M.; Suzuki, W.; Fujiwara, E.; Tanaka, H.; Tokumoto, M.; Okano, Y.; Fujiwara, H.; Kobayashi, H. *J. Am. Chem. Soc.* **2004**, *126*, 426−427. (f) Fujiwara, E.; Kobayashi, A.; Fujiwara, H.; Kobayashi, A. *Inorg. Chem.* **2004**, *43*, 1122−1129. (g) Sasa, M.; Fujiwara, E.; Kobayashi, A.; Ishibashi, S.; Terakura, K.; Okano, Y.; Fujiwara, H.; Kobayashi, H. *J. Mater. Chem.* **2005**, *15*, 155−163. (h) Kubo, K.; Nakao, A.; Yamamoto, H. M.; Kato, R. *J. Am. Chem. Soc.* **2006**, *128*, 12358−12359.
(4) (a) Kumasaki, M.; Tanaka, H.; Kobayashi, A. *J. Mater. Chem.* **1998**, *8*, 301−307. (b) Ueda, K.; Goto, M.; Iwamatsu, M.; Sugimoto, T.; Endo, S.; Toyota, N.; Yamamoto, K.; Fujita, H. *J. Mater. Chem.* **1998**, *8*, 2195−2198. (c) Ueda, K.; Kamata, Y.; Iwamatsu, M.; Sugimoto, T.; Fujita, H. *J. Mater. Chem.* **1999**, *9*, 2979−2983. (d) Rovira, C.; Novoa, J. J.; Mozos, J. L.; Ordejón. P.; Canadell, E. *Phys. Rev.* **2002**, *B65*, 081104(R). (e) Suzuki, W.; Fujiwara, E.; Kobayashi, A.; Fujishiro, Y.; Nishibori, E.; Takata, M.; Sakata, M.; Fujiwara, H.; Kobayashi, H. *J. Am. Chem. Soc.* **2003**, *125*, 1486−1487. (f) Tanaka, H.; Tokumoto, M.; Ishibashi, S.; Graf, D.; Choi, E. S.; Brooks, J. S.; Yasuzuka, S.; Okano, Y.; Kobayashi, H.; Kobayashi, A. *J. Am. Chem. Soc.* **2004**, *126*, 10518−10519. (g) Zhou, B.; Shimamura, M.; Fujiwara, E.; Kobayashi, A.; Higashi, T.; Nishibori, E.; Sakata, M.; Cui, H.; Takahashi, K.; Kobayashi, H. *J. Am. Chem. Soc.* **2006**, *128*, 3872−3873. (h) Ji, Y.; Zhang, R.; Li, Y. J.; Li, Y. Z.; Zuo, J. L.; You, X. Z. *Inorg. Chem.* **2007**, *46*, 866−873. (i) Fujiwara, E.; Yamamoto, K.; Shimamura, M.; Zhou, B.; Kobayashi, A.; Takahashi, K.; Okano, Y.; Cui, H.; Kobayashi, H. *Chem. Mater.* **2007**, *19*, 553−557.

10.1021/ic070264n CCC: $37.00
Published on Web 07/18/2007

Scheme 1

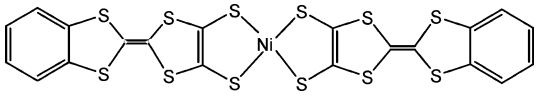

The satisfactory, but still not perfect, match between observed and calculated data is due to the low resolution caused by poor crystallinity. Complex $[Ni(btdt)_2]$ is almost isostructural with $[Ni(tmdt)_2]$. The triclinic unit cell contains only one molecule. The central Ni atoms are on the lattice points, and the four S atoms surrounding the Ni atom yield a square-planar geometry. The bond distances and angles are within the normal range. The whole molecule is ideally planar. It is noteworthy that there are many shorter S···S contacts and $\pi\cdots\pi$ interactions between neighboring molecules, indicating that the system has three-dimensional intermolecular interactions (Figure 1).

However, there is a crucial difference in molecular packing between $[Ni(btdt)_2]$ and $[Ni(tmdt)_2]$. In $[Ni(btdt)_2]$, all of the neighboring molecules are in slipped stacking along the shorter molecular axis, which is common for the nickel dithiolate complex with extended TTF ligands, such as $[Ni(C_{10}H_{10}S_8)_2]$,[3a] $[Ni(ptdt)_2]$,[3b] and $[Ni(hfdt)_2]$.[3g] However, for $[Ni(tmdt)_2]$, the neighboring molecules are somewhat "dimerized" and form a zigzag column structure along the stacking direction (Figure 2).

The absorption spectrum for the solid powder sample of $[Ni(btdt)_2]$ shows a broad absorption maximum at ca. 5500 cm^{-1} (1820 nm), which is much larger than that observed in $Ni(tmdt)_2$ (ca. 2200 cm^{-1}; 4540 nm).[2c,3g] Electrical conductivity measurement using compressed pellets over the range 80−293 K (Figure 3) reveals that $[Ni(btdt)_2]$ is a narrow-gap semiconductor with a room-temperature conductivity of 10 S cm^{-1}. This value is significantly lower than that of $[Ni(tmdt)_2]$ (200 S cm^{-1} for the powder sample). Upon cooling, the electrical resistivity increases gradually from 300 to 200 K and then increases sharply when the temperature is further lowered.

The electronic structure of $[Ni(btdt)_2]$ was calculated under both the local density approximation and generalized gradient approximation using SVP or 6-31g(d,p) basis sets (see the Supporting Information for details). The optimized molecule

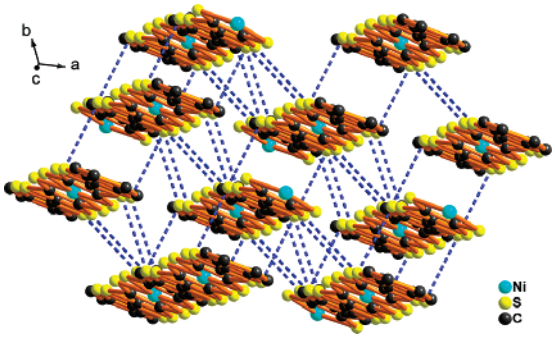

Figure 1. Packing diagram of complex $[Ni(btdt)_2]$ (dotted lines representing S···S nonbonded contacts of less than 3.60 Å).

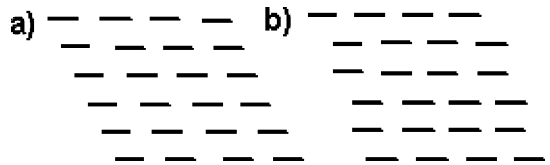

Figure 2. Packing diagram of complexes $[Ni(btdt)_2]$ (a) and $[Ni(tmdt)_2]$ (b).

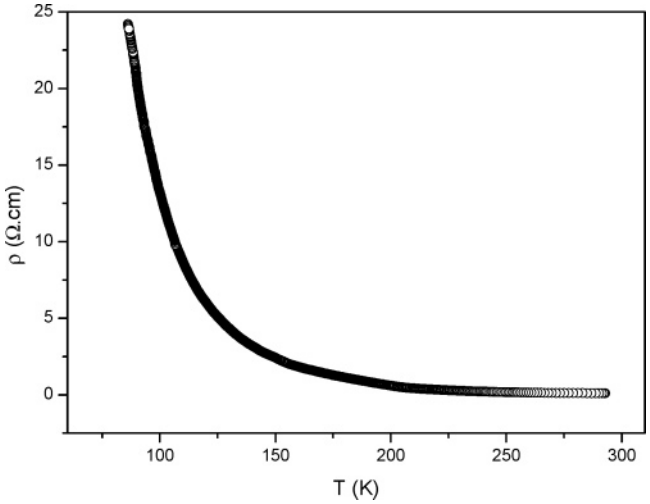

Figure 3. Temperature dependence of the electrical resistivity of $[Ni(btdt)_2]$.

structure had a good planarity with D_{2h} symmetry. The highest occupied molecular orbital (HOMO) and lowest unoccupied molecular orbital (LUMO) of $[Ni(btdt)_2]$ are π-like orbitals with b_{3u} and b_{2g} symmetries, respectively, with a very small HUMO−LUMO energy gap (0.405−0.478 eV). Interestingly, the HOMO−LUMO energy gap of $[Ni(btdt)_2]$ is very close to that of $[Ni(tmdt)_2]$ (calculated to be 0.371−0.430 eV in our study), suggesting that the HOMO−LUMO energy gap is not the key factor for the electrical conducting property.

Since the molecular HOMO−LUMO energy gap is practically identical, the reason for the large difference in the conductivity between $[Ni(btdt)_2]$ and $[Ni(tmdt)_2]$ is perhaps due to the difference in molecular packing. Extend Hückel tight-binding calculations were performed to obtain the band structure of $[Ni(btdt)_2]$ in two types of packing modes, as shown in Figure 2 (see the Supporting Information for calculation details). For stacking a, the HOMO and LUMO bandwidths were estimated to be 0.266 and 0.198 eV,

(5) The PXRD pattern of $[Ni(btdt)_2]$ (**2**) was indexed using the program DICVOL (Boultif, A.; Löuer, D. *J. Appl. Crystallogr.* **2004**, *37*, 724−731), giving the triclinic unit cell with $a = 6.6102$ Å, $b = 7.2322$ Å, $c = 12.8340$ Å, $\alpha = 89.58°$, $\beta = 93.03°$, $\gamma = 112.311°$, and $V = 566.767$ Å^3. The structure was solved using a parallel tempering approach implemented in the program FOX (Favre-Nicolin, V.; Cerny, R. *J. Appl. Crystallogr.* **2002**, *35*, 734−743. FOX, *"free objects for crystallography": A modular approach to ab initio structure determination from powder diffraction*). Rietveld refinements were alternated with Fourier difference maps, using the GSAS program (Larson, A. C.; Von Dreele, R. B. *General Structure Analysis System (GSAS)*; Los Alamos National Laboratory Report LAUR 86-748; Los Alamos National Laboratory, Los Alamos, NM, 2004).

(6) Final Rietveld refinement results for $[Ni(btdt)_2]$ (**2**): $M_r = 691.70$, triclinic, space group $P\bar{1}$, $a = 6.7203(16)$ Å, $b = 7.3808(12)$ Å, $c = 12.5627(33)$ Å, $\alpha = 87.141(21)°$, $\beta = 93.624(35)°$, $\gamma = 111.799(12)°$, $V = 577.17(22)$ Å^3, $Z = 1$, $\rho = 1.964$ g cm^{-3}, $R_P = 0.0843$, $R_{wP} = 0.1253$, $R_F = 0.0824$, R_{wP}(expected) $= 0.0658$, for 3850 data points collected in the range of $3° \le 2\theta \le 60°$, where $R_P = \sum|y_{obs} - y_{calc}|/\sum|y_{obs}|$; $R_{wP} = [\sum w(y_{obs} - y_{calc})^2/\sum w(y_{obs})^2]^{1/2}$; $R_F = \sum|F_o - F_c|/\sum F_o$, $R_{exp} = [(N - P1 - P2)/\sum w(y_{obs})^2]^{1/2}$.

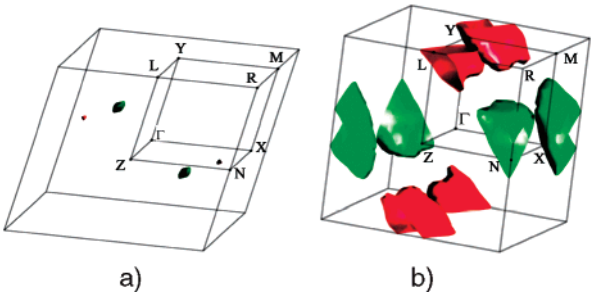

Figure 4. Hole (green) and electron (red) Fermi surfaces of $[Ni(btdt)_2]$ in different packing modes. $\Gamma = (0, 0, 0)$, $X = (1/2, 0, 0)$, $Y = (0, 1/2, 0)$, $Z = (0, 0, 1/2)$, $M = (1/2, 1/2, 0)$, $N = (1/2, 0, 1/2)$, $L = (0, 1/2, 1/2)$, and $R = (1/2, 1/2, 1/2)$, in units of the triclinic reciprocal lattice vectors.

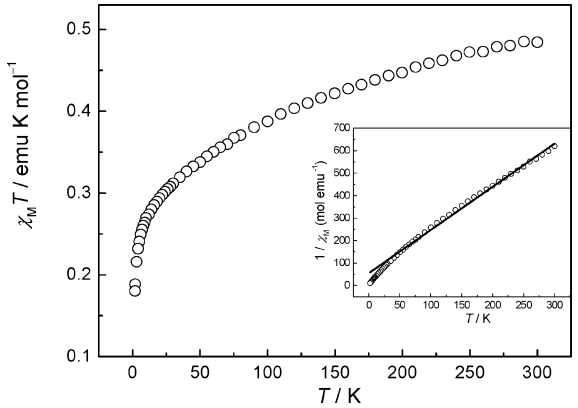

Figure 5. Temperature dependence of $\chi_m T$ for $[Ni(btdt)_2]$. The inset is $1/\chi_m$ vs T. The solid line corresponds to the best fit to the Curie−Weiss law.

respectively. There is no overlap between the HOMO and LUMO bands (Figure S10a in the Supporting Information). Only very small electron and hole pockets were obtained on the Fermi surface (Figure 4a). This result is consistent with the observed semiconducting property of $[Ni(btdt)_2]$. However, when the $[Ni(btdt)_2]$ molecules are "dimerized" (stacking b), the calculated HOMO and LUMO bandwidths were 0.291 and 0.262 eV, respectively. The two bandwidths had an overlap of 0.06 eV (Figure S10b in the Supporting Information). Large electron and hole pockets were obtained on the Fermi surface (Figure 4b), indicating a metallic conducting behavior. According to the previous studies on TTF-like single-component metals, the HOMO and LUMO often form a "crossing band" whose Fermi surface tends to vanish because of the HOMO−LUMO interactions. Only very small electron and hole pockets appeared in the Fermi surface as a result of the transverse interaction between neighboring columns. A large Fermi surface can only be obtained when large transverse intermolecular interactions are observed in a three-dimensional system. Therefore, the absence of "dimerization" of $[Ni(btdt)_2]$ molecules weakens the transverse intermolecular interactions and the HOMO−LUMO interactions destroy the Fermi surface, thus resulting in the difference of electrical properties.

The electron spin resonance spectra of $[Ni(btdt)_2]$ were recorded in the solid state at 120 and 298 K (Figure S7 in the Supporting Information). At 298 K, one weak broad doublet signal was observed at $g = 2.011$. At 120 K, the broad signal was sharpened with g values of 2.007. The magnetic susceptibility variations in different temperatures of $[Ni(btdt)_2]$ were measured in 1.8−300 K (Figure 5). At room temperature, its $\chi_M T$ value is 0.48 emu K mol^{-1}, which is smaller than the spin-only value of 0.75 emu K mol^{-1} ($S = 1$) for the radical in the π-conjugated dithiolate units and the unpaired electron in the Ni^{III} ions without any exchange coupling. With decreasing temperature, between 300 and 20 K, the $\chi_M T$ values exhibit a quasi-linear dependence with T from 0.48 to 0.29 emu K mol^{-1} and then decrease smoothly below ca. 10 K, reaching a minimum value of 0.18 emu K mol^{-1} at 1.8 K. The magnetic susceptibility above 25 K obeys the Curie−Weiss law with the Curie (C) and Weiss (θ) constants $C = 0.52$ emu K mol^{-1} and $\theta = -28.63$ K, suggesting that intermolecular antiferromagnetic coupling is dominant in the complex. This is reasonable because there are many short intermolecular S···S contacts and $\pi-\pi$ stacking interactions as described above.

In conclusion, the neutral nickel complex with a highly π-conjugated dithiolate ligand, benzotetrathiafulvalenedithiolate, shows a high conductivity at room temperature. The structural analysis from PXRD experiments shows that it has a different packing mode from that of $[Ni(tmdt)_2]$, which leads to the variance of conductivity. The results are reasonable and consistent with our computational results.

Acknowledgment. This work was supported by the National Natural Science Foundation of China (Grants 20531040 and 20473095), the Major State Basic Research Development Program (Grant 2006CB806104), the Program for New Century Excellent Talents in University of China (Grant NCET-04-0469), and the Natural Science Foundation of Jiangsu Province (Grant BK2006512).

Supporting Information Available: Synthesis, more magnetic data, details of the crystal structure determination from powder X-ray diffraction data, and X-ray crystallographic data in CIF format. This material is available free of charge via the Internet at http://pubs.acs.org.

IC070264N